


Resolving Ultrafast Spin-Orbit Dynamics in Heavy Many-Electron Atoms

Jack Wragg,^{*} Daniel D. A. Clarke, Gregory S. J. Armstrong, Andrew C. Brown,
Connor P. Ballance, and Hugo W. van der Hart

*Centre for Theoretical Atomic Molecular and Optical Physics, School of Mathematics and Physics,
Queen's University Belfast, Belfast BT7 1NN, Northern Ireland, United Kingdom*

 (Received 15 April 2019; revised manuscript received 9 July 2019; published 15 October 2019)

We use R -matrix with time-dependence theory, with spin-orbit effects included, to study krypton irradiated by two time-delayed extreme ultraviolet ultrashort pulses. The first pulse excites the atom to $4s^24p^55s$. The second pulse then excites $4s4p^65s$ autoionizing levels, whose population can be observed through their subsequent decay. By varying the time delay between the two pulses, we are able to control the excitation pathway to the autoionizing states. The use of cross-polarized light pulses allows us to isolate the two-photon pathway, with one photon taken from each pulse.

DOI: [10.1103/PhysRevLett.123.163001](https://doi.org/10.1103/PhysRevLett.123.163001)

Since the genesis of attosecond light pulses, nearly 20 years ago, great strides have been made in understanding how electronic motion can be observed and manipulated in a variety of atomic and molecular processes [1,2]. Most of this understanding has been developed for systems involving light atoms, where the influence of relativistic interactions such as spin-orbit coupling is assumed to be sufficiently weak to be negligible over the timescales of interest. However, a number of recent advances have opened opportunities of harnessing spin-orbit effects to enable a deeper understanding of electron dynamics, including the observation of spin-orbit dependent effects in subcycle electron dynamics in ionization from atoms by a near-infrared pulse [3], effects in attosecond-timescale ionization [4], and time delays in photoemission [5].

This deeper understanding of spin-orbit interactions may also enhance our ability to manipulate the electron dynamics. For example, it has been shown that in ionization from atoms, the spin polarization of the ejected electrons can be controlled using circularly polarized light fields in conjunction with the spin-orbit interaction [6]. Moreover, many important biological processes such as photoreception and photosynthesis depend on population transfer between spin multiplicities mediated by the spin-orbit interaction [7].

Despite these advances, the need for theoretical methods that are able to provide a complete description of spin-orbit interaction dynamics persists. Some steps have already been taken in this direction. For example, it has been shown that it is possible to account for spin-orbit effects using modified single-active-electron models [8], and analytic techniques such as the strong-field approximation [9], Perelomov-Popov-Terent'ev theory [10,11], and the analytical R -matrix method [12]. One of the most advanced methods is the time-dependent configuration-interaction singles approach [13]. However, even this does not fully incorporate all characteristics of the spin-orbit interaction,

as only its angular aspect is considered from first principles, with energy effects accounted for through empirical energy shifts [12,13].

As a candidate for the full study of spin-orbit interaction, we propose the use of R -matrix with time-dependence (RMT) theory. Over the past decade, RMT has been established as one of the premier methods for the investigation of ultrafast dynamics in multielectron systems. This theory builds upon the standard R -matrix theory for scattering, which was amended for the treatment of heavier atomic systems through the development of the Breit-Pauli R -matrix approach [14]. In this Letter, we demonstrate that by adopting the Breit-Pauli R -matrix approach within time-dependent R -matrix theory we can extend RMT to describe ultrafast processes in heavy atoms which include relativistic effects.

We demonstrate the capability of this semirelativistic RMT approach through application to an example experimentally relevant problem: the combined effect of two time-delayed ultrafast laser pulses to induce two-photon excitation of an autoionizing state in Kr (see Fig. 1). Here, the first laser pulse (duration 6 cycles, photon energy 10 eV, and peak intensity 10^{13} W/cm²) excites the Kr atom from the $4s^24p^6$ 1S ground state to $4s^24p^55s$ $^1P^o$. Then, spin-orbit coupling within the $4p^5$ core will transfer population to the $4s^24p^55s$ $^3P^o$ state and back on a timescale given by the splitting between the levels within $4s^24p^55s$. The second time-delayed laser pulse (duration 6 cycles, photon energy 15 eV, and peak intensity 10^{12} W/cm²) then excites the Kr atom from $4s^24p^55s$ to $4s4p^65s$ 1S_0 and 3S_1 states, which will subsequently autoionize. By varying the time delay between the pulses, we can control the excitation to these autoionizing states. For both 6 cycle pulses, we employ a \sin^2 profile, indicating 3 cycles of ramp on immediately followed by 3 cycles of ramp off. We use a

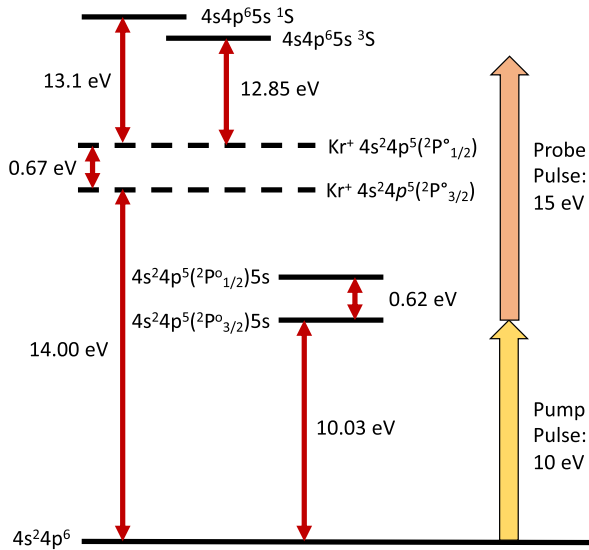


FIG. 1. Energy levels of atomic krypton relevant to the autoionization process shown in Fig. 2 (not to scale).

cosine function for the carrier frequency of each pulse, such that unphysical effects resulting from an overall nonzero pulse displacement (e.g., as described in Ref. [15]) are avoided.

In pump-probe schemes such as this, ionization can typically occur through a vast number of pathways. Any number of photons can be absorbed from either pulse, and all paths interfere with one another. This interplay of interfering pathways can obscure the physics of direct interest, and has manifested itself in previous work (see, e.g., Fig. 6 in Ref. [16], where a fast oscillatory change in ionization is superimposed on the ionization yield of interest). To bring the physics of interest to the fore, it is thus important to find schemes that isolate specific pathways. A benefit of the use of RMT is that it accounts for the combined effect of all pathways by design, so it is possible to investigate which factors enhance the signal from pathways of interest. In this study, we examine the effect of varying the polarization direction of the second pulse. We find this affords selectivity in this combined excitation-ionization scheme, enabling the resolution of processes that might otherwise interfere and hide the signal from the physics of interest. Furthermore, we find that this use of cross-polarized pulses allows the results to be interpreted in terms of the dynamics within the electron hole, driven by the spin-orbit interaction.

This work employs a similar scheme to that previously developed by Wörner and Corkum [17], which described the effect of spin-orbit interaction induced dynamics associated with a superposition of $P_{1/2}$ and $P_{3/2}$ states in noble gas ions. These dynamics can then be observed through measurement of the ionization rate under a further ionization step. Later works were able to observe these effects experimentally [18,19]. Here, our use of RMT

theory allows the inclusion of a greater number of possible processes in the model, broadening the range of the physics we are able to study. Specifically, in the present work we modify the scheme to involve an autoionizing state, allowing the physics of interest to occur within the neutral krypton atom without requiring a further ionization step. The autoionizing state of interest (i.e., $4s4p^65s$) has been previously studied experimentally from a time-independent perspective [20].

We use the RMT method (for a full description, see Refs. [21,22]) to solve the time-dependent Schrödinger equation,

$$i \frac{\partial}{\partial t} \Psi(\mathbf{X}, t) = [\hat{H}_A + \hat{H}_{SO} + \hat{H}_D(t)] \Psi(\mathbf{X}, t), \quad (1)$$

where \mathbf{X} indicates spin and spatial dimensions for all electrons, \hat{H}_A is the field-free atomic Hamiltonian, and \hat{H}_{SO} is the Breit-Pauli spin-orbit interaction applied to all electrons. $\hat{H}_D(t)$ is the time-dependent dipole operator which describes the interaction of the laser with all electrons. To implement \hat{H}_{SO} we require semirelativistic atomic data input, which we obtain from the fully *ab initio*, and widely used, RMatrixI package [14,23,24]. Hence all aspects of the spin-orbit interaction are taken into account, including the effect on both the angular and radial aspects of the wave function.

We build a model krypton atom, in which we include the $4p^{-1}$ and $4s^{-1}$ residual ion configurations. Bound orbitals are taken from preexisting Hartree-Fock calculations [25], and we represent the continuum orbitals with a basis of 50 B splines of order 9, extending up to the inner region boundary at $20a_0$. We obtain a Kr model with a ground state spin-orbit splitting in the residual ion of 0.668 eV (experiment gives 0.666 eV [26]), and ionization potential from the krypton atom ground state of 13.42 eV (experiment gives 14.00 eV [26]). This model contains 29 electron emission channels when the spin-orbit interaction is omitted, and 66 channels when it is included. We retain all symmetries up to total orbital angular momentum $L = 8$ when the spin-orbit interaction is omitted, and total angular momentum $J = 8$ when included. For the cross-polarized pulses study, we include symmetries up to $M_J = 3$, increasing the number of channels to 800. We propagate the wave function up to a final time of 47 fs (the duration of each pulse is 2.44 fs), allowing plenty of time for ionized wave packets to escape the atomic core. We use a time step of 0.2 as, and describe the ejected electron up to a distance of $2168a_0$ from the core.

Figure 2 shows ejected electron spectra in the region corresponding to decay from the relevant autoionizing state, for cases where the two pulses are parallel polarized [2(a)] and cross-polarized [2(b)]. We show spectra calculated using time delays of 4, 5, and 6 fs between the two pulses. In all spectra we see two peaks, which can be

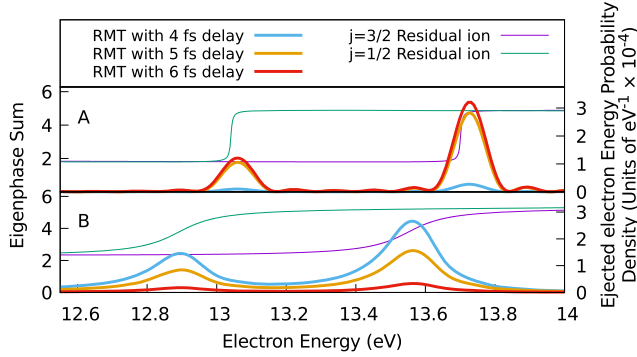


FIG. 2. Ejected electron spectra for delays of 4, 5, and 6 fs between the two pulses. We show results for when the pulses are parallel polarized (a) and cross-polarized (b). We also show the corresponding eigenphase sum calculated using the same Kr model using the RMatrixI time-independent codes. In the upper frame we plot the eigenphase sum for the $J = 0$ even symmetry, and in the lower frame we show that for $J = 1$ even symmetry, to indicate the position of the resonances for parallel- and cross-polarized pulses, respectively.

explained by the spin-orbit splitting of the $4s^24p^5$ residual ion state: the $4s4p^65s$ autoionizing state decays to either $4s^24p^5\ ^2P_{1/2}^o$ or $^2P_{3/2}^o$. This is supported by the energy gap between the two peaks matching the splitting of these two states (0.66 eV).

For comparison, in Fig. 2, we also include a time-independent $\text{Kr}^+ + e^-$ electron scattering calculation using the same krypton model. Here, we plot two versions of the eigenphase sum such that the peaks correspond to the decay signal from resonant states (i.e., we shift the spectra corresponding to decay to $j = \frac{1}{2}$ by 0.66 eV). As parallel-polarized pulses will excite to 1S , and cross-polarized pulses will excite to 3S (as discussed below), we plot the eigenphase sum in the $J = 0$ even symmetry to compare with the parallel-polarized spectra, and we plot the $J = 1$ even symmetry to compare with data obtained from cross-polarized pulses. We see that all peaks in the RMT spectra can be matched with the $4s4p^65s$ autoionizing resonances found in the time-independent calculation. The small difference in energy between the RMT and time-independent peaks (approximately 0.025 eV) is ascribed to the potential energy experienced by the RMT wave packets, as a residual field persists even at these large distances.

From the spectra in Fig. 2, we can obtain a measure of the population of the autoionized state by integrating over the peaks of interest. Inevitably this will introduce dependence on calculation length, as it is impractical to propagate to a time where the autoionizing state can be considered to be fully decayed. While it might be possible to obtain quantitative results through fitting to an exponential decay, in this work we are most interested in the short-time dynamical effect of the time delay between the pulses rather than the absolute population autoionized. Thus we

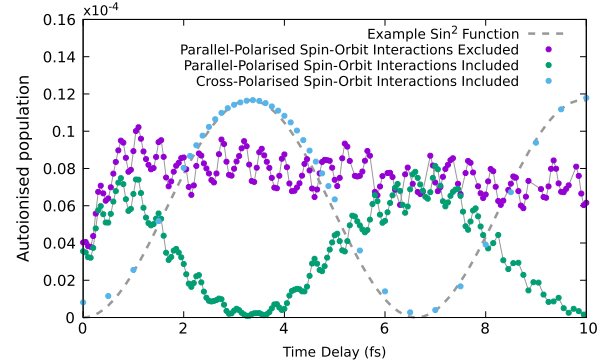


FIG. 3. Measure of ionization resulting from the decay of the $4s4p^65s$ state excited by a 6 cycle 10 eV pulse followed by a 6 cycle 15 eV pulse after a specified time delay. The population is calculated at a time of 47 fs after the start of the first pulse. We plot results for parallel-polarized cases where the spin-orbit interaction is omitted, and parallel-polarized and cross-polarized cases for when the spin-orbit interaction is included. We also plot a \sin^2 function (dashed gray line) of the frequency associated with the 0.615 eV splitting, of amplitude scaled to fit the cross-polarized dataset.

simply report the weight of the peak as measured at the end of the calculation.

One of the most striking features of the results in Fig. 2 is the dependence of the weight of the peak on the time delay between the two pulses. We expand this result in Fig. 3 to plot the autoionized population (i.e., the area under the peaks) for a scan over a wider range of time delays. We first focus attention on the case where both pulses are polarized in the same direction. To show the effect of the spin-orbit interaction, we calculate datasets where the spin-orbit interaction is included and omitted. On the longer time-scale, the spin-orbit interaction introduces a strong periodic modulation on the degree of autoionization from the atom. When the spin-orbit interaction is omitted, however, this periodicity disappears. We attribute this periodic behavior to the splitting of the $4s^24p^55s$ state into the $^2P_{1/2}^o$ and $^2P_{3/2}^o$ core states. To support this explanation, we note that this longer oscillation has a period corresponding to approximately 0.62 eV (demonstrated by the corresponding gray dashed line), matching the splitting between the $4s^24p^5(^2P_{1/2}^o)5s$ and $4s^24p^5(^2P_{3/2}^o)5s$ levels with $J = 1$ [26].

To further explain this oscillation, we present similar results obtained using cross-polarized pulses in Fig. 3. These results show an identical periodicity, but are out of phase with the results obtained using parallel-polarized pulses. To explain this phase difference, we consider these results in an uncoupled electron basis and the corresponding selection rules in Fig. 4. Here the dynamics are considered in three stages. Stage A shows the ground state of the krypton atom, in which a $4p_0$ electron is excited to $5s_0$ by a pulse polarized in the z direction (following the

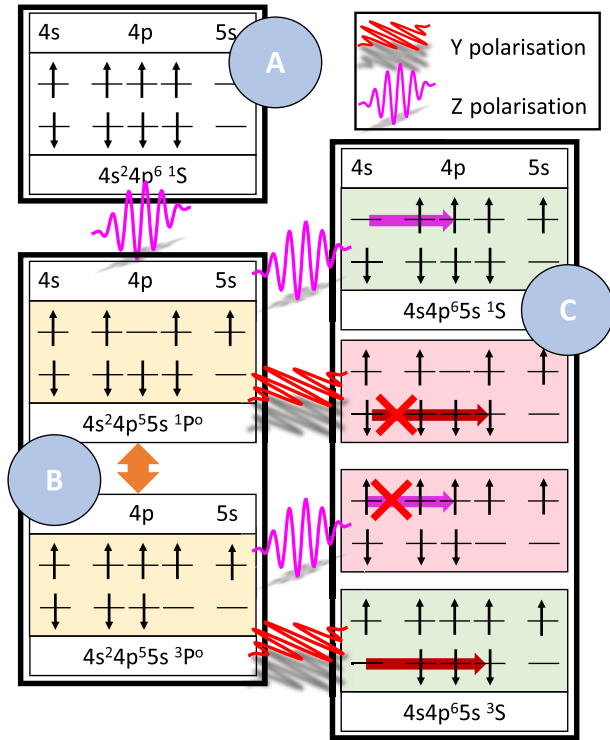


FIG. 4. A schematic to demonstrate the electron dynamics displayed in Fig. 3 in an uncoupled electron basis, shown in three stages (large blue circles). In stage A, the ground state krypton atom is excited by a 10 eV pulse. Stage B shows the effect of the spin-orbit interaction upon the $4p$ hole, and stage C shows the effect of the second 15 eV pulse for parallel-polarized and cross-polarized pulses. See text for more detail.

selection rule on the electron magnetic quantum number $\Delta m_\ell = 0$). Stage B then shows the effect of the spin-orbit interaction, which moves the hole from $4p_0$ to $4p_{\pm 1}$ and back again. Thus, by varying the time delay we control the location of the hole state which is probed by the second pulse.

Stage C shows the effect of the second pulse, where a 15 eV photon attempts to excite a $4s$ electron to $4p$, and form the $4s 4p^6 5s$ autoionizing state. The success of this process depends on whether the transition is allowed given the location of the hole and the selection rules of the second pulse. For example, a z -polarized pulse ($\Delta m_\ell = 0$) will excite the $4s_0$ electron to $4p_0$ only when there exists a $4p_0$ hole. If this is the case, then the autoionizing state will form and its decay can be observed. If, however, there is no $4p_0$ hole, the autoionizing state cannot be reached. Similarly, a y -polarized pulse ($\Delta m_\ell = \pm 1$) can only excite the $4s_0$ electron to a $4p_{\pm 1}$ hole. If this hole does not exist at the time of excitation, the autoionizing state cannot be reached.

With this perspective, the sinusoidal behavior in Fig. 3 can be interpreted as representing the time-varying location of the $4p$ hole. When the parallel-polarized pulses show a maximum in the observed autoionization decay, the hole can be considered to be in $4p_0$. Correspondingly, when the

cross-polarized pulses show a maximum, the hole can be considered to be in $4p_{\pm 1}$.

In addition to the slow oscillation, both sets of parallel-polarized data display a fast oscillation with time delay which is absent in the cross-polarized data (we note that a numerical origin of this oscillation has been ruled out through careful checks). We attribute this oscillation to interference between three excitation pathways: the main pathway of interest which requires the absorption of a single photon from each pulse, and two other pathways, where two photons are absorbed from either of the pulses.

We again consider the dipole selection rules, here in terms of M_J (i.e., $\Delta M_J = 0$ for z -polarized pulses, $\Delta M_J = \pm 1$ for y -polarized pulses). When two photons are absorbed from the same pulse, insufficient time elapses between photon absorptions for the spin-orbit interaction to affect the spin of a core electron. These excitation paths must thus result in excitation of the $4s 4p^6 5s^1 S_0$ state. In the parallel-polarized case, therefore, the dipole selection rules ensure all pathways yield the same final state, and thus the pathways can interfere. However, in the cross-polarized case the pathway of interest (one photon delivered by each pulse) gives a $4s 4p^6 5s^1 S_1$ final state such that the pathway of interest no longer interferes with the others, and we do not observe the fast oscillation in the autoionization yield. This explanation is supported by the frequency of the fast oscillation. While the oscillation does not seem to be purely sinusoidal, its dominant frequency is approximately 10 eV, which corresponds to the energy gap between the first excited state and the ground state.

In the cross-polarized case, we can thus isolate the excitation process of interest from the main interfering pathways. We note that previously published pump-probe results looking at spin-orbit effects seem to contain the same type of fast oscillations which could be attributed to similar interference effects (see, e.g., Fig. 1 in Ref. [19]). This shows how the wide range of processes included in the RMT approach enables a close representation of experiment, allowing these more subtle effects to be uncovered. Using the laser polarization to select specific pathways as we have done here could be realized as an effective method for resolving different processes in experiment. In this particular case, it also removes apparent “noise” which might otherwise obscure the signal of interest. We intend to further analyze this effect in a follow-up paper.

We fully expect that despite current technological limitations, this phenomenon should be observable in experiment. The autoionization mechanism is mediated entirely by single-photon processes, and thus limited laser intensity is not an issue. Furthermore, varying the relative pulse polarization to isolate specific ionization or excitation pathways does not face any technological barrier as far as we are aware. The most pressing limitation is the ability to create sufficiently short laser pulses in the extreme ultraviolet (XUV) regime. An high-harmonic generation

source is the most promising candidate and it can be expected that the current drive towards XUV-pump-XUV-probe experiments will bring even the parameters discussed in this Letter within reach [27,28].

To summarize, we have developed an *ab initio* Breit-Pauli R -matrix with time-dependence approach and applied it to model ionization from a krypton atom subject to two ultrafast laser pulses. We found that it is possible to control the m_ℓ of a core hole at the moment of the second pulse by varying the time delay between the pulses. The state of this core can be measured by exciting the atom to an auto-ionizing state with the second pulse, and observing the resulting decay.

Through the demonstration of these effects, we have shown the importance of spin-orbit effects in *ab initio* calculations. While inclusion of the spin-orbit interaction can increase the computational resources required by the calculation, it is important that simulations of electron behavior do not naively assume it is not required. Furthermore, we have shown how the Breit-Pauli approach can be combined with the RMT approach for arbitrary polarization. Specifically, we demonstrate the potential for exploitation of spin-orbit effects in the observation and control of electron dynamics using parallel- and cross-polarized excitation schemes. These results give hope that further schemes to control electron dynamics at the level of the spin-orbit interaction may be possible. For instance, similar behavior could be observed in more complex systems (e.g., molecules), where spin-orbit splitting occurs on similar energies, and hence dynamics occurs on similar timescales.

The data presented in this Letter may be accessed online [29]. The RMT code is part of the UK-AMOR suite, and can be obtained online for free [30].

We acknowledge Jakub Benda and Zdeněk Mašín for their collaboration in developing and maintaining the RMT code. This work benefited from computational support by CoSeC, the Computational Science Centre for Research Communities, through CCPQ. D. D. A. C. acknowledges financial support from the UK Engineering and Physical Sciences Research Council (EPSRC). A. C. B., H. W. v. d. H., G. S. J. A., and J. W. acknowledge funding from the EPSRC under Grants No. EP/P022146/1, No. EP/P013953/1, and No. EP/R029342/1. This work relied on the ARCHER UK National Supercomputing Service [31], for which access was obtained via the UK-AMOR consortium funded by EPSRC.

*jack.wragg@qub.ac.uk

[1] F. Krausz and M. Ivanov, *Rev. Mod. Phys.* **81**, 163 (2009).
 [2] F. Calegari, G. Sansone, S. Stagira, C. Vozzi, and M. Nisoli, *J. Phys. B* **49**, 062001 (2016).

[3] M. Sabbar, H. Timmers, Y.-J. Chen, A. K. Pymer, Z.-H. Loh, S. G. Sayres, S. Pabst, R. Santra, and S. R. Leone, *Nat. Phys.* **13**, 472 (2017).
 [4] A. Wirth, M. T. Hassan, I. Grguraš, J. Gagnon, A. Moulet, T. T. Luu, S. Pabst, R. Santra, Z. Alahmed, A. Azzeer *et al.*, *Science*, **334**, 195 (2011).
 [5] I. Jordan, M. Huppert, S. Pabst, A. S. Kheifets, D. Baykusheva, and H. J. Wörner, *Phys. Rev. A* **95**, 013404 (2017).
 [6] A. Hartung, F. Morales, M. Kunitski, K. Henrichs, A. Laucke, M. Richter, T. Jahnke, A. Kalinin, M. Schöffler, L. P. H. Schmidt *et al.*, *Nat. Photonics* **10**, 526 (2016).
 [7] W. Rettig, *Angew. Chem. Int. Ed. Engl.* **25**, 971 (1986).
 [8] I. A. Ivanov and A. S. Kheifets, *Phys. Rev. A* **89**, 043405 (2014).
 [9] D. B. Milošević, *Phys. Rev. A* **93**, 051402(R) (2016).
 [10] A. M. Perelomov, V. S. Popov, and M. V. Terent'ev, *Sov. Phys. JETP* **23**, 924 (1966).
 [11] I. Barth and O. Smirnova, *Phys. Rev. A* **88**, 013401 (2013).
 [12] J. Kaushal and O. Smirnova, *J. Phys. B* **51**, 174003 (2018).
 [13] S. Pabst and R. Santra, *J. Phys. B* **47**, 124026 (2014).
 [14] K. A. Berrington, W. B. Eissner, and P. H. Norrington, *Comput. Phys. Commun.* **92**, 290 (1995).
 [15] I. A. Ivanov, A. S. Kheifets, K. Bartschat, J. Emmons, S. M. Buczek, E. V. Gryzlova, and A. N. Grum-Grzhimailo, *Phys. Rev. A* **90**, 043401 (2014).
 [16] M. A. Lysaght, H. W. van der Hart, and P. G. Burke, *Phys. Rev. A* **79**, 053411 (2009).
 [17] H. J. Wörner and P. B. Corkum, *J. Phys. B* **44**, 041001 (2011).
 [18] A. Fleischer, H. J. Wörner, L. Arissian, L. R. Liu, M. Meckel, A. Rippert, R. Dörner, D. M. Villeneuve, P. B. Corkum, and A. Staudte, *Phys. Rev. Lett.* **107**, 113003 (2011).
 [19] L. Fechner, N. Camus, J. Ullrich, T. Pfeifer, and R. Moshammer, *Phys. Rev. Lett.* **112**, 213001 (2014).
 [20] J. Baxter and P. Mitchell, *J. Comer, J. Phys. B* **15**, 1105 (1982).
 [21] L. Moore, M. Lysaght, L. Nikolopoulos, J. Parker, H. Van Der Hart, and K. Taylor, *J. Mod. Opt.* **58**, 1132 (2011).
 [22] D. D. A. Clarke, G. S. J. Armstrong, A. C. Brown, and H. W. van der Hart, *Phys. Rev. A* **98**, 053442 (2018).
 [23] C. Ramsbottom, C. Ballance, R. Smyth, A. Conroy, L. Fernández-Menchero, M. Turkington, and F. Keenan, *Galaxies* **6**, 90 (2018).
 [24] R. Smyth, C. Ramsbottom, F. Keenan, G. Ferland, and C. Ballance, *Mon. Not. R. Astron. Soc.* **483**, 654 (2019).
 [25] E. Clementi and C. Roetti, *At. Data Nucl. Data Tables* **14**, 177 (1974).
 [26] E. B. Saloman, *J. Phys. Chem. Ref. Data* **36**, 215 (2007).
 [27] M. Fushitani, Y. Hikosaka, A. Matsuda, T. Endo, E. Shigemasa, M. Nagasono, T. Sato, T. Togashi, M. Yabashi, T. Ishikawa, and A. Hishikawa, *Phys. Rev. A* **88**, 063422 (2013).
 [28] T. Barillot, P. Matia-Hernando, D. Greening, D. Walke, T. Witting, L. Frasinski, J. Marangos, and J. Tisch, *Chem. Phys. Lett.* **683**, 38 (2017).
 [29] <https://doi.org/10.17034/660e22b1-4130-4a51-95c0-0781c6061f1d>.
 [30] <https://gitlab.com/Uk-amor/RMT>.
 [31] <http://www.archer.ac.uk/>.